Int. J. Heat Mass Transfer. Vol. 28, No. 5, pp. 919–928, 1985
Printed in Great Britain

0017–9310/85 $3.00 + 0.00

A study of binary mixture boiling: boiling site density and subcooled heat transfer

T. O. HUI and J. R. THOME
Department of Mechanical Engineering, Michigan State University, U.S.A.

(*Received* 9 *December* 1983 *and in final form* 27 *August* 1984)

Abstract—Boiling site densities and heat-transfer coefficients have been measured for ethanol–water and ethanol–benzene mixtures at 1.01 bar for a heated vertical brass disk. A strong effect of composition on the boiling site density was observed, which was attributed to the nature of the activation of the boiling surface and mass diffusion effects. The boiling heat-transfer coefficient was found to decrease with increasing subcooling, but for the mixtures at a given level of subcooling the decrease was less than that for the single components and azeotropic mixtures. The heat-transfer coefficient at a given heat flux was seen to be quite insensitive to the very large increase in boiling site density in comparing the pure water and the ethanol–water azeotrope results, leading one to question pool boiling models that predict heat-transfer rates on the basis of boiling site density.

1. INTRODUCTION

NUCLEATE pool boiling of liquid mixtures is distinct from single component boiling in that their heat-transfer coefficients can be considerably lower than those of an equivalent pure fluid with the same physical properties as the actual mixtures. Previous investigators have attributed this reduction in heat transfer performance to be caused by: (a) a rise in the local boiling point due to preferential evaporation of the more volatile component during bubble growth [1], (b) a significant change in the mixture physical properties with composition [2, 3], (c) the effect of composition on nucleation [2, 4, 5, 6], and (d) the retardation of the principle heat-transport mechanisms [7].

Physical intuition leads one to believe that the three identifiable heat-transport mechanisms responsible for the large boiling heat-transfer coefficients (bubble microlayer evaporation, cyclic thermal boundary-layer removal, and bubble-induced convection) are directly linked to the number of active boiling sites on the heated surface. Thus, the present study seeks to determine the effects of composition and subcooling on the boiling site density to investigate its contribution to the degradation in the heat-transfer performance. Consequently, heat-transfer coefficients and boiling site densities were obtained simultaneously in the experiments to be reported here.

Previous experimental work on boiling site density in binary liquid mixtures was performed by Van Stralen and is summarized in [8]. His tests covered several aqueous systems. Only one study included data for each of the constituent single component liquids to permit the comparison with the one mixture composition tested, 4.1 wt% methyl ethyl ketone (MEK) in water. The test section in that study was a 0.2 mm diameter wire. At a heat flux of 300 kW m^{-2} it was observed that the number of active boiling sites cm^{-2} in pure water was 30 and in MEK over 200, but for the 4.1% MEK mixture only one site was active. Hence, a substantial effect of composition was evident.

The effect of subcooling on the nucleate pool boiling curves of benzene–diphenyl mixtures has been investigated by Sterman *et al.* [9], who used nitrogen gas to obtain subcoolings up to 80 K. They found that the mixture heat-transfer coefficients based on a wall superheat calculated using the bulk liquid temperature (note that some researchers use the bulk saturation temperature instead) decreased with increased subcooling, as occurs in single component boiling. The mixture heat-transfer coefficients were observed to decrease with subcooling less than those of the two single components.

2. EXPERIMENTAL APPARATUS AND METHODS

Pool boiling facility

A schematic diagram of the boiling rig is shown in Fig. 1. The insulated pressure vessel is a stainless-steel cross with flanged ends. To maintain the desired temperature and pressure inside the vessel, a proportional-type temperature controller connected to an immersion heater and a water-cooled condenser are used. In cases where the bulk test liquid is maintained in a subcooled state, nitrogen gas is fed into the vessel using a pressure regulator so that the system pressure is maintained at 1.01 ± 0.02 bar, the pressure at which all experiments were run.

The test section is mounted vertically facing a sight glass window for photographic purposes. Heat is provided by a specially designed electrical resistance heater attached firmly to the back side of the 1.0 inch (25.4 mm) diameter brass test surface. The test surface was prepared before each experimental run by rubbing with a fine emery paper (silicon carbide 320) and then finished with crocus paper. A portion of the outer part

NOMENCLATURE

N/A	boiling site density [sites cm^{-2}]
$\dot{q}$	heat flux [kW m^{-2}]
T	saturation temperature [°C]
ΔT	wall superheat [K]
ΔT_{sub}	subcooling [K]
$\tilde{x}$	liquid mole fraction
$\tilde{y}$	vapor mole fraction.

Greek symbols

α	heat-transfer coefficient [kW m^{-2} K^{-1}]
α_I	ideal heat-transfer coefficient [kW m^{-2} K^{-1}]
$\Delta 0$	rise in local boiling point [K].

Subscripts

az	azeotrope
b	bulk
eth	ethanol.

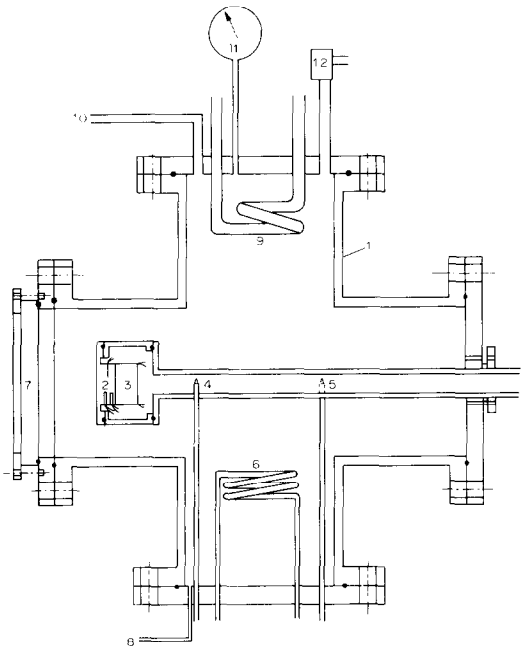

FIG. 1. Nucleate pool boiling rig. (1) Stainless-steel insulated vessel; (2) test surface and thermocouples; (3) electric heater; (4) bulk liquid thermocouple; (5) temperature controller thermocouple; (6) immersion heater; (7) sight glass window; (8) liquid fill line; (9) condenser; (10) valve to vacuum pump/atmosphere/gas bottle; (11) pressure gauge; (12) safety relief valve.

of the test section was made very thin (0.4 mm) to minimize the conductive heat losses in the radial direction. A circle of 19.1 mm diameter was lightly inscribed at the center of the test surface for use in determining the boiling site density.

The test surface temperature was obtained by linear extrapolation of the temperatures measured by the two thermocouples located closest to the surface (Fig. 1). Copper–constantan thermocouple wires were used to form the thermocouple junctions. The bulk liquid temperature was measured using another thermocouple placed at the same height as the test section, as also depicted in Fig. 1. A digital thermocouple readout device was used for the temperature measurements and the thermocouple readings were periodically checked for agreement when no heat flux was applied to the test surface. The electrical power dissipated was determined by measuring the DC current and voltage applied by a Hewlett–Packard power supply to the resistance heater. The voltage was measured with local sensing leads and a digital multimeter. The DC current was monitored across a precision $0.001 \pm 1\%\,\Omega$ shunt. The heat flux passing through the 1.0 inch (25.4 mm) diameter test surface was corrected for heat conducted out through the thin fin. The error in the heat flux so determined was estimated to be about $\pm 5\%$ while the error in the wall superheat is ± 0.3 K.

Test liquids

Ethanol–water and ethanol–benzene mixtures were chosen for the present test fluids. Ethanol–water mixtures have a large variation in surface tension and contact angle with composition, so that a significant effect of composition on boiling site density was anticipated. On the contrary, the physical properties of ethanol–benzene mixtures do not change dramatically and hence only a slight effect on boiling side density was expected.

Double-distilled water and reagent grades of ethanol and benzene were used to prepare the test liquids. The liquid mixtures were prepared on a weight basis corresponding to the mole fraction desired. The liquid mixture thus obtained had an accuracy of ± 0.015 mole fraction. The liquid composition was also checked by measuring its density after the experimental run.

Photographic method

A Canon A-1 camera with motordrive and a photographic lamp were used to obtain still photographs of the boiling test surface through the sight glass window. Three photographs were obtained for each set of experimental conditions, i.e. mixture composition, heat flux and subcooling.

For each active boiling site on the heated surface the

boiling cycle can be divided into the bubble growth time and the waiting time. Since the vapor nucleus is too small to be seen in the photograph during the waiting time, a counting of the boiling site density from any single photograph would underestimate the actual number of sites. Therefore, three separate photographs were taken at different instants of time and the following scheme was used to reduce this error in the counting procedure.

During the counting of each photograph a piece of paper is placed directly underneath it. The counting is done by punching a tiny hole in the center of the bubble. Thus the location of a bubble attached to the surface is also recorded on this piece of paper. This procedure is repeated for the two other photographs, being careful to align the paper properly. The number of active boiling sites within the inscribed circle is then obtained by counting the holes in the paper. The accuracy of this method, which is estimated to be about $\pm 20\%$, includes an error estimate associated with borderline cases in which it is not clear whether or not the bubble is attached to the surface.

Experimental procedures

After introducing the test liquid into the vessel and bringing it to the boiling point, the liquid is degassed by opening a vent to the atmosphere. Then the power to the resistance heater is turned on and gradually increased to a heat flux of about 150 kW m^{-2}, at which level vigorous boiling occurs on the test surface. The power is then lowered successively to the six heat fluxes tested and the appropriate data and photographs are obtained when steady-state conditions are reached under each condition. The liquid temperature is then lowered 5 K to the next level of subcooling while nitrogen gas is injected to maintain the pressure at 1.01 bar. The heat flux is again raised to 150 kW m^{-2} and the same procedure is followed until all subcoolings have been achieved.

A more detailed discussion of the experimental apparatus and experimental methods are given in Hui [10].

3. BOILING SITE DENSITY RESULTS

Ethanol–water mixtures

Measurements of boiling site densities were made at six heat flux levels ranging from 14 to 97 kW m^{-2} and subcoolings of 0 to 20 K. Boiling site densities were not attainable in all cases due to too much interaction between bubbles, preventing accurately distinguishing among individual bubbles.

Figure 2 shows an example of the boiling surface photographed for a 0.15 mole fraction of ethanol in water at a heat flux of 97 kW m^{-2}, a wall superheat of 29.4 K, and 10 K of subcooling.

Figure 3 depicts the results for boiling site density at a constant heat flux of 97 kW m^{-2}. The values range from about 10 sites cm^{-2} for pure water up to 400 sites cm^{-2} at the azeotrope composition, with the values increasing rapidly as the mole fraction passes 0.5. At saturation conditions the boiling site density was always found to be too high to distinguish individual bubbles. As the subcooling rose, the bubbles attached

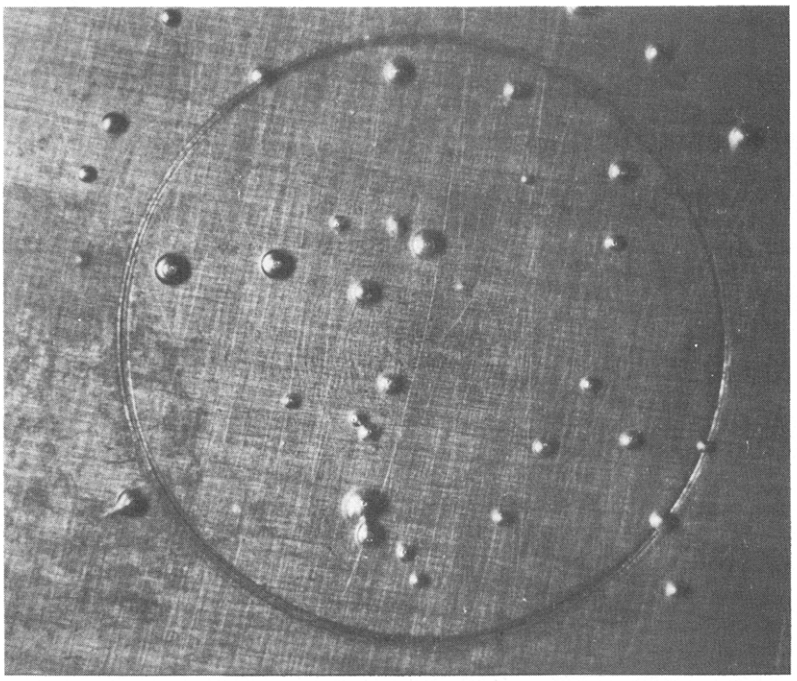

FIG. 2. Photograph of heated surface showing boiling of an ethanol–water mixture ($\bar{x}_{eth} = 0.15$; $\dot{q} = 97$ kW m^{-2}; $\Delta T = 29.4$ K; $\Delta T_{sub} = 10.0$ K).

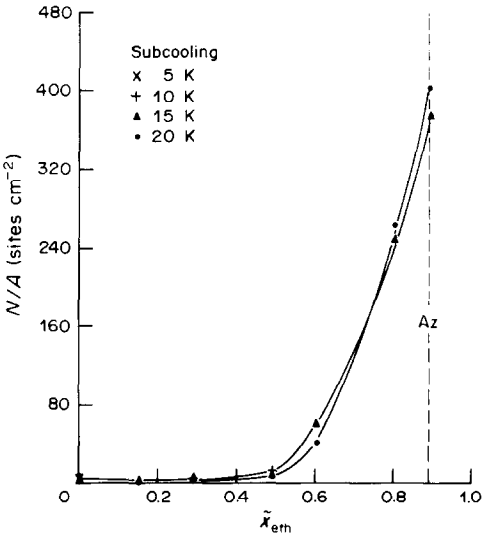

FIG. 3. Boiling site density for ethanol–water mixtures at 97 kW m^{-2} and various subcoolings.

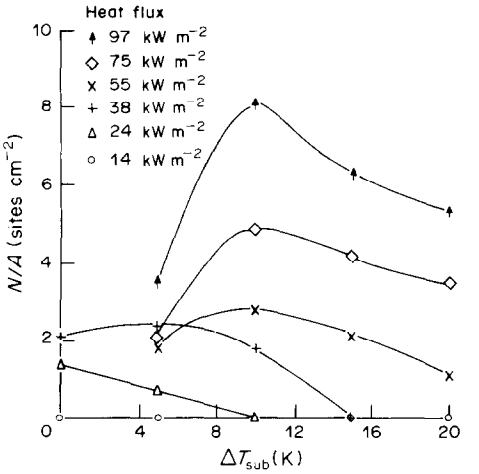

FIG. 5. Boiling site density as a function of subcooling at various heat fluxes for $\tilde{x}_{eth} = 0.29$.

to the surface become more visible. The site density values are observed to be much less than expected by a simple linear molar interpolation between the water and azeotrope values and are consistent with the Van Stralen results for water–MEK mixture.

The effect of subcooling on the boiling site density is demonstrated in Fig. 4 for a mixture with a mole fraction of 0.60. The site density (N/A) is seen to decrease monotonically as the subcooling increases at all heat flux levels. Some mixtures also exhibited a maximum in the N/A value with respect to subcooling as shown in Fig. 5 for a 0.29 mole fraction mixture. Figure 6 shows the variation in boiling site density with heat flux for a 0.80 mole fraction mixture.

Ethanol–benzene mixtures

A typical photograph of the boiling in an ethanol–benzene mixture is shown in Fig. 7. The test liquid is 0.30 mole fraction ethanol. The heat flux is 55 kW m^{-2}, while the wall superheat is 17.8 K and subcooling of 5 K exists. Figure 8 depicts the boiling site density data obtained at 97 kW m^{-2}. A minimum occurs to the right of the azeotrope while a maximum is observed to the left

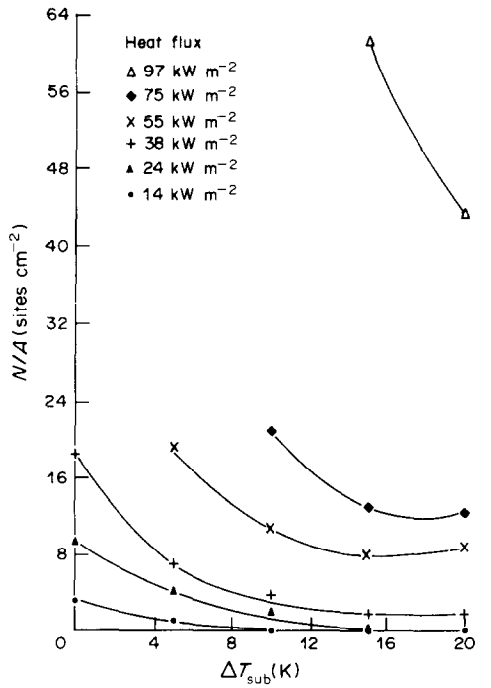

FIG. 4. Boiling site density as a function of subcooling at various heat fluxes for $\tilde{x}_{eth} = 0.60$.

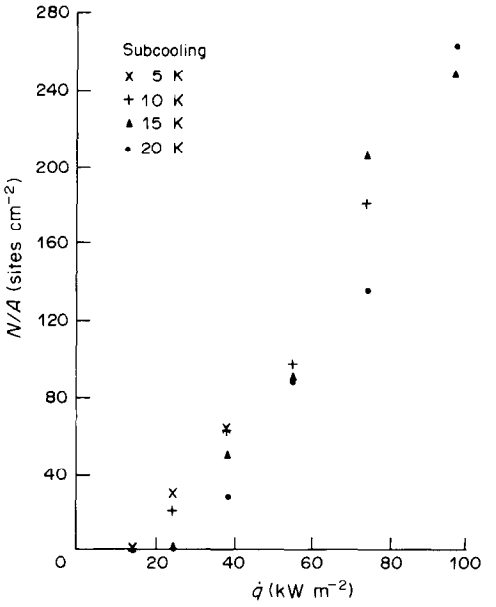

FIG. 6. Variation in boiling site density with heat flux at various subcoolings for $\tilde{x}_{eth} = 0.80$.

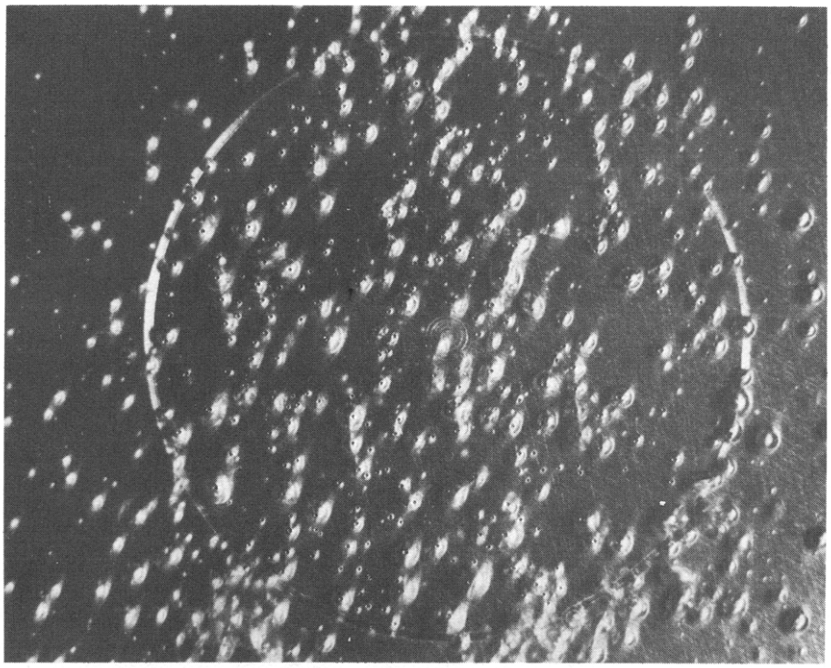

FIG. 7. Photograph of the heated surface showing boiling of an ethanol–benzene mixture ($\tilde{x}_{eth} = 0.30$; $\dot{q} = 55$ kW m^{-2}; $\Delta T = 17.8$ K; $\Delta T_{sub} = 5.0$ K).

at subcoolings of 15 and 20 K. By contrast, at a heat flux of 55 kW m^{-2}, the maximum for these subcoolings has shifted to the azeotrope composition as observed in Fig. 9. At the 10 K subcooling level, the maximum has shifted to a mole fraction of 0.30 ethanol.

Figure 10 shows the boiling site density plotted vs subcooling for an 0.80 mole fraction ethanol mixture. At low heat fluxes little change is seen to occur but at 97 kW m^{-2} a shallow minimum is observed. The variation of boiling site density with heat flux is depicted in Fig. 11 for a 0.45 mole fraction mixture, i.e. the azeotrope. The trend is similar to Fig. 6.

4. HEAT TRANSFER

Ethanol–water mixtures

The effects of composition and subcooling on the heat-transfer coefficient are shown in Figs. 12 and 13. A very profound minimum in the heat-transfer coefficient is evident at saturation conditions but becomes very

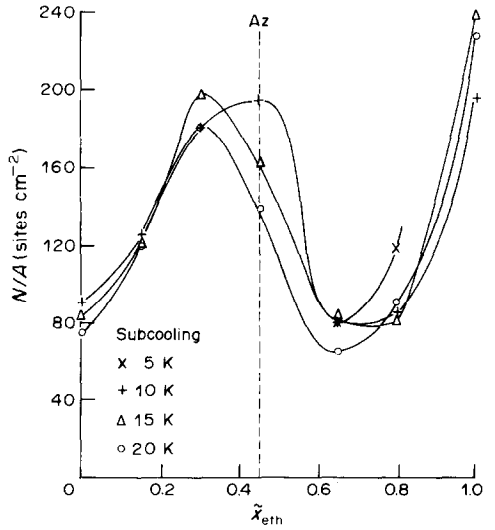

FIG. 8. Boiling site density for ethanol–benzene mixtures at 97 kW m^{-2} and various subcoolings.

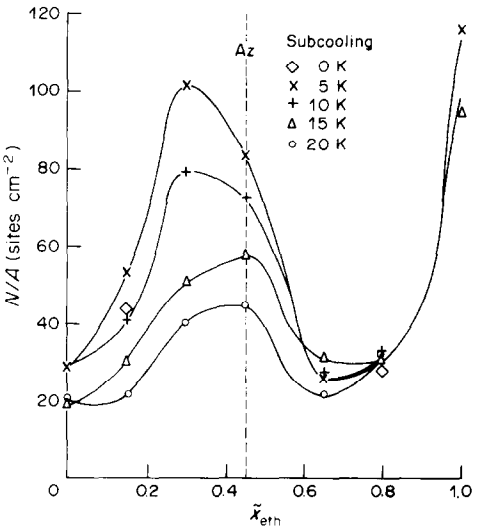

FIG. 9. Boiling site density for ethanol–benzene mixtures at 55 kW m^{-2} and various subcoolings.

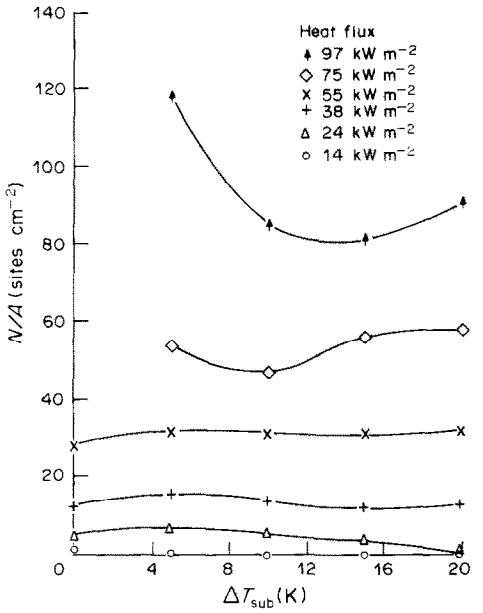

FIG. 10. Boiling site density as a function of subcooling at various heat fluxes for $\tilde{x}_{eth} = 0.80$.

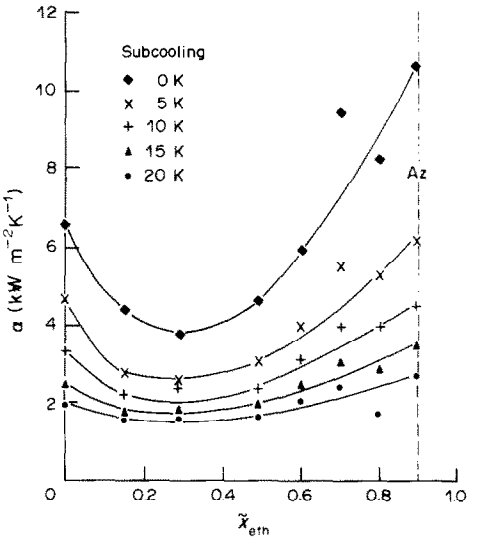

FIG. 12. Boiling heat-transfer coefficient as a function of composition for ethanol–water mixtures at 97 kW m^{-2} and various subcoolings.

shallow at a subcooling of 20 K. Figure 14 shows the decrease in the heat-transfer coefficient at the various heat flux levels with increasing subcooling for a 0.60 mole fraction mixture. The absolute drop in α is much greater at the higher heat fluxes but the percentage decreases from 0 to 20 K subcooling are essentially the same for all heat fluxes.

Ethanol–benzene mixtures

Figures 15 and 16 present the heat-transfer data at two heat fluxes. The minimum in the heat-transfer coefficient at either side of the azeotrope becomes less profound with increasing subcooling which is similar to the ethanol–water results. For a 0.80 mole fraction mixture, the effect of subcooling is shown in Fig. 17.

5. DISCUSSION

The large rise in the boiling site density shown in Fig. 3 for mole fractions greater than 0.5 is explainable by the two different modes of activation of the boiling surface. An increase in the wall superheat required to

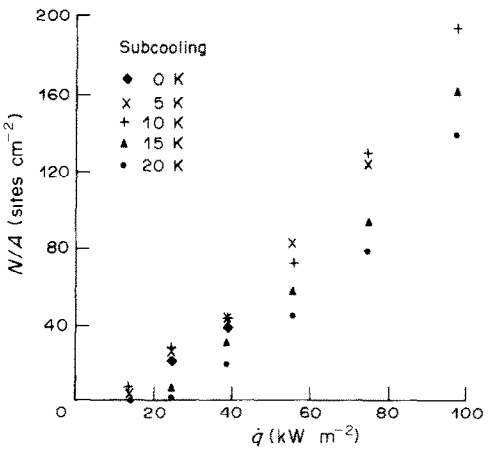

FIG. 11. Variation in boiling site density with heat flux at various subcoolings for $\tilde{x}_{eth} = 0.45$, the azeotrope composition.

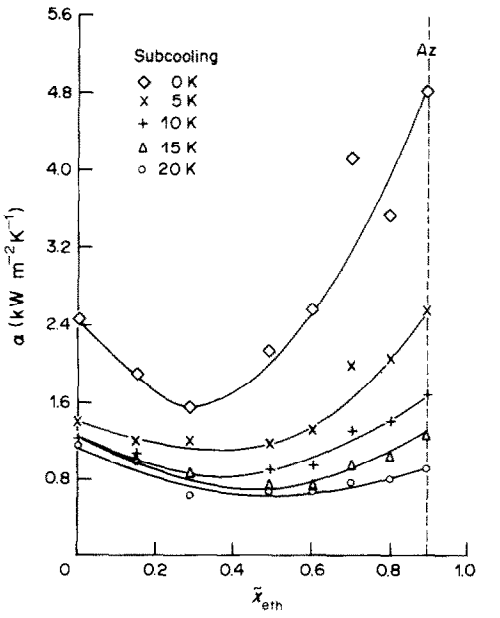

FIG. 13. Boiling heat-transfer coefficient as a function of composition for ethanol–water mixtures at 38 kW m^{-2} and various subcoolings.

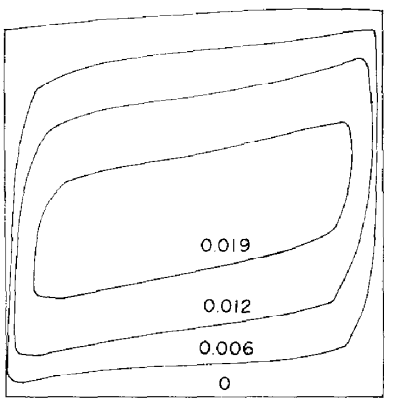

FIG. 4. Streamlines for $Ra = 1000$ with $\varepsilon = 0.5$.

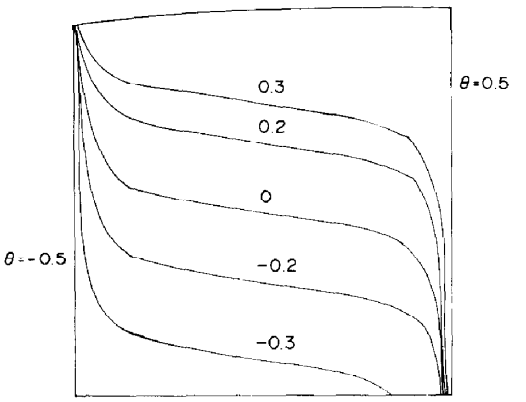

FIG. 5. Isotherms for $Ra = 1000$ with $\varepsilon = 0.5$.

for $\varepsilon = 0.5$; Nu was also calculated for the case of a fixed top. We have not been able to find values for Nu for the fixed top in the literature, so we do not have anything to compare our results with. In Figs. 2–5 streamlines and isotherms are plotted for Ra equal to 200 and 1000 with $\varepsilon = 0.5$ and $\gamma = 1$.

5. DISCUSSION

The study presented in this paper had two purposes. The first one was to develop a numerical procedure for solving such a highly nonlinear problem. The problem is nonlinear in two different ways; the field equations are coupled through the nonlinear convective terms in the heat conduction equations, and in addition the boundary conditions on the free surface are nonlinear. The results we obtained indicate that the numerical procedure works and is reasonably accurate. However, we have not been able to find any other published results to compare them with.

The second purpose of the study was to explore the effects of the free surface. The results in Table 1 show that the maximum depth of the saturated part of the slab increases by 8% for $Ra = 50$ while for $Ra = 1000$ the increase is 3% compared with the fixed top case. The conclusion we can draw from Table 2 is that the Nusselt number is not really dependent on the free surface; at least not at the accuracy with which these calculations were carried out.

Acknowledgements—The research by one of the authors (H.R.) is supported financially by NSERC (Grant No. A9251).

REFERENCES

1. E. B. Hansen and H. Rasmussen, Steady free surface flow in a porous slab heated from its sides, *Utilitas Mathematica* **23**, 281–292 (1983).
2. P. D. F. Liu and J. A. Liggett, Boundary integral solutions to ground water problems, in *Applied Numerical Modelling* (Proceedings edited by C. A. Brebbia), pp. 557–569 (1978).
3. H. Rasmussen and D. Salhani, Unsteady porous flow with a free surface, *IMA J. Appl. Math.* **27**, 307–318 (1981).
4. R. J. Ribando and K. E. Torrance, Natural convection in a porous medium: effects of confinement, variable permeability, and thermal boundary conditions, *Trans. Am. Soc. Mech. Engrs*, Series C, *J. Heat Transfer* **98**, 42–48 (1976).
5. D. K. Gartling, Finite element analysis of convective heat transfer in a porous medium, *Proc. 3rd Int. Conf. on Finite Elements in Flow Problems*, Banff, Canada, pp. 194–203 (1978).
6. M. A. Havstad and P. J. Burns, Convective heat transfer in vertical cylindrical annuli filled with a porous medium, *Int. J. Heat Mass Transfer* **25**, 1755–1766 (1982).

LA SURFACE LIBRE SUR UN LIQUIDE QUI REMPLIT UNE COUCHE POREUSE CHAUFFEE SUR SES COTES

Résumé—On calcule numériquement la position de la surface libre pour une couche poreuse qui est partiellement remplie par un liquide et qui est chauffée de façon différente sur ses cotés. Une transformation de coordonnées est utilisée pour transformer le système physique du problème original en un système non orthogonal où la surface libre devient une ligne droite fixe. Le problème transformé est alors résolu en utilisant une méthode aux différences finies. Des résultats sont obtenus pour des nombres de Rayleigh allant jusqu'à 1000.

the higher ethanol compositions the wall superheat is relatively large and the activation of the first boiling site appears to simultaneously activate the entire heated surface. Thus, the usual nucleation criteria seems to apply only to the first site and a different phenomenon apparently is responsible for activation of the other sites. It is speculated by the present authors that the adjacent cavities may be filled with vapor as the dry patches underneath the growing neighboring bubbles pass over them. With the additional vapor, they now have larger radii and may nucleate. Also, the effect of the suction created by the departure wake of the first large, rapidly growing bubble is perhaps sufficient to locally superheat the microlayer due to the locally decreased pressure (like the decompression of a chamber with a moving piston), causing the vapor nuclei to activate as a result of the larger superheat thus produced.

The question then arises as to why the 0.60 mole fraction mixture has a much smaller boiling site density than the azeotropic mixture when both were activated by the same process. This is probably due to mass diffusion effects. Consider that with the rapid generation of vapor at the surface, the local boiling point rises due to the preferential evaporation of the more volatile component (see Fig. 18). Hence, the vapor nucleus left behind by a departing bubble has a composition of $\tilde{y}$ rather than $\tilde{y}_b$. The incoming bulk liquid has a composition of $\tilde{x}_b$, which means the vapor nucleus is supersaturated with respect to the less volatile component (water). Since mass diffusion in the vapor phase is much more rapid than in the liquid phase, this component tends to condense out to achieve phase equilibrium. This decreases the radius of the vapor nucleus and may cause deactivation of the boiling site (a process similar to subcooling a pure fluid). This effect becomes more important as $(\tilde{y}_b - \tilde{x}_b)$ increases. The minimum to the right of the azeotrope for ethanol–benzene mixtures shown in Figs. 8 and 9 may also be explained by the foregoing rationale.

It is generally thought that contact angle and surface tension play a strong role in determining the boiling site density. The ethanol–water system has a significant variation in these properties while ethanol–benzene does not. Hence, their effects do not seem to be clear here since both systems display large minima in N/A.

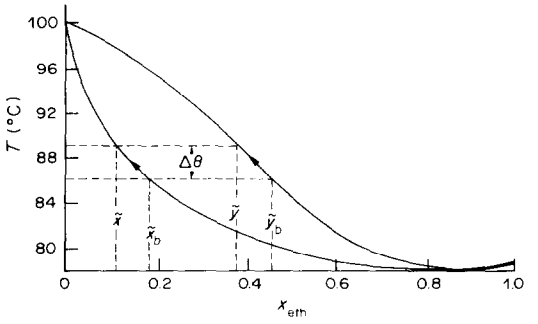

FIG. 18. Phase equilibrium diagram for ethanol–water at 1.01 bar showing the rise in the local boiling point, $\Delta\theta$.

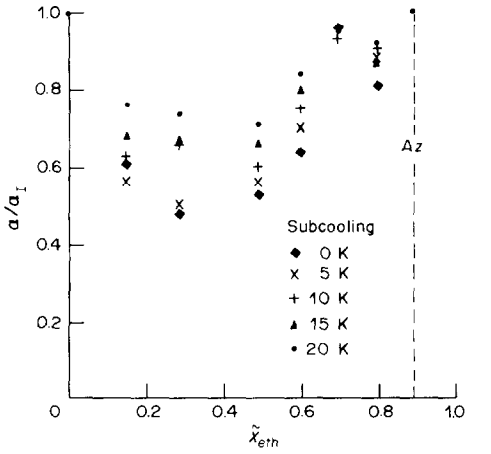

FIG. 19. The variation in the heat-transfer coefficient from ideality at various subcoolings for ethanol–water mixtures with $\dot{q} = 97$ kW m^{-2}.

For ethanol–benzene compositions to the left of the azeotrope the trend in the boiling site density is not consistent and suggests another undertermined factor is affecting the boiling site density. The maxima in N/A at 0.30 mole fraction ethanol at subcoolings of 15 and 20 K at 97 kW m^{-2} in Fig. 8 are shifted to the azeotrope in Fig. 9 at 55 kW m^{-2}. At an even lower heat flux of 24 kW m^{-2} (not shown), minima are observed at subcoolings of 10, 15 and 20 K. Consequently, the activation and deactivation process seems to be more complex than as briefly outlined above.

The effect of subcooling on the degradiation in the heat-transfer coefficient is illustrated in Figs. 19 and 20. The actual heat-transfer coefficient α is non-dimensionalized with an idealized heat-transfer coefficient α_I obtained from a linear interpolation from the single component value to the azeotropic value at the particular subcooling. In general, the data show that as the subcooling increases, the minimum in α/α_I

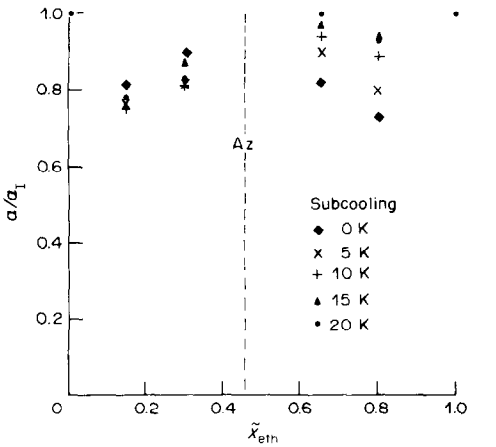

FIG. 20. The variation in the heat-transfer coefficient from ideality at various subcoolings for ethanol–benzene mixtures with $\dot{q} = 97$ kW m^{-2}.

becomes less profound. This can be explained as follows. First, the portion of the energy transfer by single-phase natural convection becomes more significant as the degree of subcooling increases. Also, the vapor bubbles begin to condense at or near the heated wall as the subcooling increases. The rise in the local saturation temperature due to the stripping of the more volatile component from the liquid is less at higher subcoolings because the excess of the more volatile component in the vapor bubble is reintroduced into the liquid phase nearer the wall. Consequently, there is less reduction in the heat-transfer coefficient due to mass diffusion effects as the level of subcooling rises.

The idea that successful understanding of the boiling site density will lead to an accurate pool boiling model and heat-transfer equation, as intoned by the Mikic and Rohsenow correlation [12] and the Thome [13] mixture boiling model (which are based on the cyclic thermal boundary-layer stripping mechanism at an individual boiling site and the boiling site density), appears much less tenable in light of the present data. The heat-transfer coefficient is actually rather insensitive to the very large increase in N/A in going from pure water to the ethanol–water azeotrope. For example, at a heat flux of 97 kW m^{-2} and a subcooling of 15 K for ethanol–water mixtures, α increases only by about 40% while N/A increases by about 4000%! The effect of increased boiling side density has to cause thermal interference between neighboring bubbles, such that each individual bubble becomes less efficient as a transporter of heat. It should also be noted that for ethanol–water mixtures the actual boiling site density can be as little as about one-tenth of the ideal boiling site density but the actual heat-transfer coefficient is only reduced to about two-thirds the ideal value. Thus, the basic philosophy that a better understanding of the surface effects on nucleate pool boiling processes, i.e. nucleation and site density, will lead to improved predictive methods for heat-transfer coefficients is actually rather tenuous without much more precise understanding of the heat-transport mechanisms themselves.

6. CONCLUSIONS

(1) Boiling site densities and heat-transfer coefficients have been measured as a function of composition, subcooling, and heat flux for ethanol–water and ethanol–benzene mixtures.

(2) For ethanol–water and for compositions of ethanol–benzene to the right of the azeotrope, the boiling site densities were much smaller than those expected from a simple linear interpolation between the single component and azeotrope values.

(3) The nature of the activation of the boiling surface and mass diffusion effects on nucleation were proposed as the primary phenomena influencing the decrease in the boiling site density.

(4) While the effect of subcooling on mixture boiling was to decrease the heat-transfer coefficient, the reduction relative to the ideal boiling heat-transfer coefficient was less as the level of subcooling increased. Also, the reduction was less for the mixtures than those for the single components and the azeotropic composition mixtures.

(5) The heat-transfer coefficient at a given heat flux level is seen to be quite insensitive to the very large increase in boiling site density in comparing the pure water and the ethanol–water azeotrope mixture results.

Acknowledgement—Financial support for this work was provided by a grant from the National Science Foundation, CME-8006736.

REFERENCES

1. W. R. Van Wijk, A. S. Vos and S. J. D. Van Stralen, Heat transfer to boiling binary liquid mixtures, *Chem. Engng Sci.* **5**, 68–80 (1956).
2. C. V. Sternling and L. J. Tichacek, Heat transfer coefficients for boiling mixtures, *Chem. Engng Sci.* **16**, 297–337 (1961).
3. K. Stephan and P. Preusser, Heat transfer and critical heat flux in pool boiling of binary and ternary mixtures, *Ger. Chem. Engng* **2**, 161–169 (1979).
4. L. N. Grigor'ev, Studies of heat transfer of two component mixtures, *Teplo Masso Perenos* **2**, 120–127 (1962).
5. R. A. W. Shock, Nucleate boiling in binary mixtures, *Int. J. Heat Mass Transfer* **20**, 701–709 (1977).
6. K. Stephan and M. Körner, Calculation of heat transfer in evaporating binary liquid mixtures, *Chemie-Ingr-Tech.* **41**, 409–417 (1969).
7. J. R. Thome, Latent and sensible heat transport rates in the boiling of binary mixtures, *J. Heat Transfer* **104**, 474–478 (1982).
8. S. J. D. Van Stralen and R. Cole, *Boiling Phenomena*, Vol. 1, pp. 38. Hemisphere, Washington (1979).
9. L. S. Sterman, J. V. Vilemas and A. I. Abramov, On heat transfer and critical heat flux in organic coolants and their mixture boiling, *Proceedings 3rd International Heat Transfer Conference, Chicago*, pp. 258–270 (1966).
10. T. O. Hui, M.S. Thesis, Michigan State University (1983).
11. J. R. Thome, S. Shakir and C. Mercier, Effect of composition on boiling incipient superheats in binary liquid mixtures, *Proceedings 7th International Heat Transfer Conference, Munich*, Vol. 1, paper PB14 (1982).
12. B. B. Mikic and W. M. Rohsenow, A new correlation of pool-boiling data including the effect of heating surface characteristics, *J. Heat Transfer* **81**, 245–250 (1969).
13. J. R. Thome, Nucleate pool boiling of binary liquids—an analytical equation, *A.I.Ch.E. Symp. Ser.* **77**, 238–250 (1981).

ETUDE DE L'EBULLITION D'UN MELANGE BINAIRE: DENSITE DE SITES D'EBULLITION ET TRANSFERT THERMIQUE EN SOUS-REFROIDISSEMENT

Résumé—Des densités de sites d'ébullition et des coefficients de transfert ont été mesurés pour des mélanges éthanol–eau et éthanol–benzène à 1,01 bar pour un disque chauffé vertical en laiton. On observe un grand effet de la composition sur la densité de sites d'ébullition, lequel est attribué à la nature de l'activation de la surface et aux effets de diffusion massique. Le coefficient de transfert thermique décroit quand le sous-refroidissement augmente, mais pour les mélanges à un niveau donné de sous-refroidissement, la décroissance est moindre que pour les composants seuls et les mélanges azéotropiques. Le coefficient de transfert thermique à un flux donné est pratiquement insensible à un très grand accroissement de la densité de sites d'ébullition en comparaison de l'eau pure et des résultats de l'azéotrope éthanol–eau ; on est conduit à mettre en question les modèles qui prédisent des flux de transfert de chaleur sur la base de la densité de sites d'ébullition.

UNTERSUCHUNG ÜBER DAS SIEDEN BINÄRER GEMISCHE: KEIMSTELLENDICHTE UND WÄRMEÜBERGANG BEI UNTERKÜHLUNG

Zusammenfassung—An einer beheizten vertikalen Messingplatte wurden Keimstellendichte und Wärmeübergangskoeffizienten für die Gemische Äthanol–Wasser und Äthanol–Benzol bei einem Druck von 1,01 bar gemessen. Es wurde ein großer Einfluß der Gemischzusammensetzung auf die Keimstellendichte beobachtet, der auf die Natur der Heizflächenaktivierung und des Stoffdiffusioneffekts zurückzuführen ist. Der Wärmeübergangskoeffizient beim Sieden nimmt mit steigender Unterkühlung ab ; bei Gemischen ist diese Abnahme bei gleicher Unterkühlung geringer als bei den reinen Komponenten oder bei azeotropen Gemischen. Bei einer gegebenen Wärmestromdichte reagierte der Wärmeübergangskoeffizient auf eine starke Vermehrung der Keimstellendichte sehr unempfindlich, verglichen mit reinen Wasser oder azeotropen Gemischen von Äthanol und Wasser. Dies stellt Siedemodelle auf der Basis der Keimstellendichte in Frage.

ИССЛЕДОВАНИЕ КИПЕНИЯ БИНАРНОЙ СМЕСИ: ПЛОТНОСТЬ ЦЕНТРОВ ОБРАЗОВАНИЯ ПУЗЫРЬКА И ТЕПЛООБМЕН ПРИ НЕДОГРЕВЕ

Аннотация—Плотности центров образования пузырьков и коэффициенты теплообмена измерены для смесей этанол–вода и этанол–бензол при давлении 1,01 бар для нагретого вертикально расположенного латунного диска. Наблюдалось сильное влияние состава смеси на плотность центров образования пузырьков, которое обусловлено природой активации кипящей поверхности и эффектом диффузии массы. Найдено, что коэффициент теплообмена при кипении уменьшается с увеличением недогрева, но для смесей при заданном уровне недогрева уменьшение было меньше, чем для одиночных компонентов или азеотропных смесей. Обнаружено, что при заданном тепловом потоке коэффициент теплообмена совершенно нечувствителен к очень сильному росту плотности центров образования пузырьков по сравнению с результатами, полученными в опытах с чистой водой и азеотропной смесью этанол–вода, что ставит под сомнение модель кипения в большом объеме, с помощью которой рассчитывается теплообмен с учетом плотностей центров образования пузырьков.